Thermo-mechanical simulation of a magnetic pulse welding process with first experimental validations

A. DELDICQUE[a], I. GHORBEL[a]

a. ICAM, Department of Mechanical Engineering, Institut Catholique des Arts et Métiers, 6 rue Auber, 59000 LILLE, amaury.deldicque@icam.fr

Résumé :

Le cuivre est largement utilisé dans les procédés industriels de chauffage ou de refroidissement notamment en raison de ses propriétés thermiques. Pour des raisons économiques mais aussi d'optimisation de masse, l'industrie cherche à le remplacer partiellement, notamment par de l'aluminium. Le projet européen H2020 Join'Em (http:\\www.join-em.eu\) vise à la réalisation d'assemblages bi-matériaux par la technologie de soudage par impulsion magnétique. Deux cas issus de la base de données expérimentales du projet sont simulés. La méthodologie ainsi que les résultats numériques sont présentés ci-après avec confrontation éventuelle aux résultats issus de l'expérience.

Abstract:

Copper is commonly used in cooling or heating industrial processes especially due to its thermal properties. For economical reasons but also for weight optimization, industry seeks to use other materials such as aluminium. The European H2020 Join'Em project (http:\\www.join-em.eu\) aims at producing bi-materials assemblies with electromagnetic pulse welding (EMW). Two test cases extracted from the Join'Em experimental database have been simulated. The methodology and the numerical results are presented hereafter and compared to the experimental results when available.

Key words: electro-magnetic pulse welding, thermo-mechanical simulation, non linear finite element analysis, Johnson-Cook law

1 Introduction

A schematic view of the electromagnetic pulse welding process (EMW) is given below :

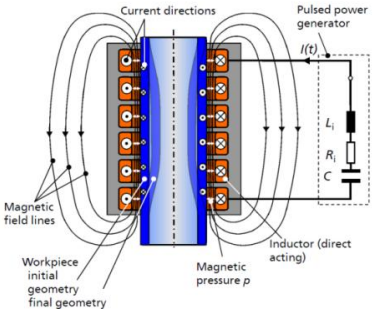

Figure 1: EMW layout [1]

Two workpieces are placed into a coil. The sudden electrical energy discharge from the capacitors into the coil creates a high intensity magnetic field which in turn induces a current in the outer workpiece and a second magnetic field of the opposite sign. As a consequence, Lorentz forces are created and a magnetic pressure is thus imposed on the outer part (the flyer plate) projecting it at a very high speed towards the inner workpiece (the fixed plate). A detailed view highlights precisely the physical phenomena that occur at the join interface:

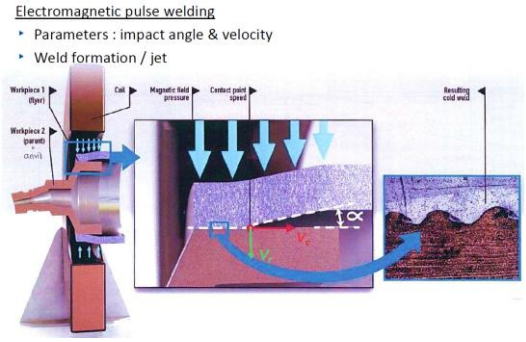

Figure 2: EMW detailed view [1]

The morphology of the interface could be straight, wavy or vortical [2]. Mainly two geometrical configurations exist : sheet welding (plane strain state) and tube welding (axisymmetric state).

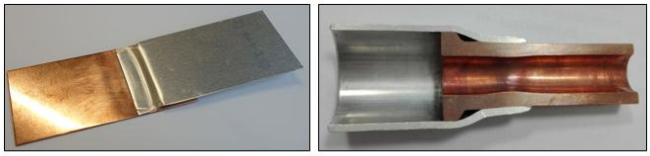

Reproduced, courtesy innovaltech Reproduced, courtesy innovaltech

Figure 3: sheet welding and tube welding

Only the first one is kept to be simulated by the finite element method. The equations to be solved by the simulation tools are the following ones:

- Mechanical Analysis

  Equilibrium equation

$$\nabla\sigma + \vec{f} = \rho\frac{\partial^2 u}{\partial t^2}$$

with the following stress/strain tensors

$\sigma = C\varepsilon^e$; $\varepsilon = \varepsilon^e + \varepsilon^p + \varepsilon^{th}$

with $\begin{cases} \varepsilon^e = \frac{1+\upsilon}{E}\sigma - \frac{\upsilon}{E}\,tr(\sigma)\mathbb{I} \\ \varepsilon^p = g(\sigma_y) \\ \varepsilon^{th} = \alpha\,(\theta - \theta_0) \end{cases}$

- Thermal Analysis

  Heat transfer equation

$$\rho\,\frac{dh}{dt} = \nabla(\lambda\nabla T) + Q_v$$

The units system used is mm/tonne/s/K

2 Numerical models description

Among the many articles dealing with EMW numerical modelling, the recent Nassiri's work [3] has been retained as a benchmark. The numerical strategy presented here provides numerical results that are closed to his results. He used Abaqus explicit and ALE formulation whereas we used MSC.Marc and Lagrangian formulation in the present work. Relying on this partial cross validation, two test cases from the Fraunhofer IWU experimental database have been simulated namely the V82 (copper to aluminium) and the V112 (aluminium to copper).

The geometry, materials properties are described below. Due to the severe deformation undergone by the materials and the related mesh distortion, remeshing techniques have been used to prevent the failure of the numerical procedure. An initial velocity of -384 m/s with an initial impact angle of 14,18° are imposed in the V82 case whereas, in the V112 case, an initial velocity of -495 m/s with an initial impact angle of 12,7° are imposed. In both cases, a room temperature is imposed for the flyer and the base as initial thermal conditions. A null displacement and a room temperature are fixed at the bottom of the base plate. A gravity load for the flyer and the base is considered for both V82 and V112 cases. Heat is generated from plastic work (conversion factor of 0.9). Regarding the material behaviour, the Johnson Cook law is used because of its temperature and strain rate sensitivities. The yield criterion is Von Mises. When contact is detected, it is supposed to be an unbreakable glue.

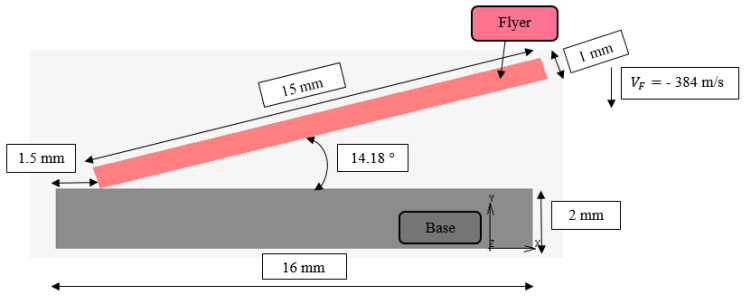

Figure 4: V82 test case

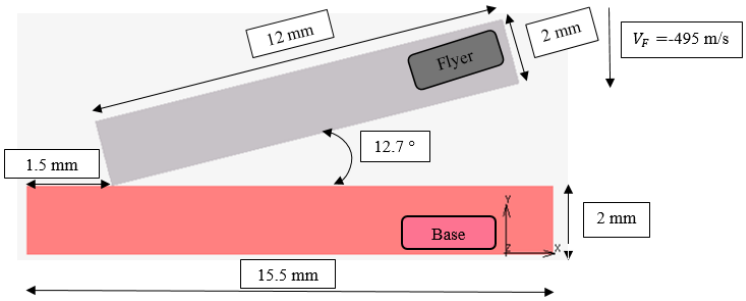

Figure 5: V112 test case

Table 1: Physical parameters

Material	$\rho(t/mm^3)$	E(MPa)	υ	K(mW/mm/K)	C_p(mJ/t/K)	α	G(MPa)
Cu-DHP	$8.5.10^{-9}$	160000	0.33	385	383.10^{6}	$1.76.10^{-5}$	60200
EN AW-1050	$2.7.10^{-9}$	69000	0.33	229	899.10^{6}	$2.33.10^{-5}$	26000

Table 2: Johnson-Cook law and associated parameters

$$\sigma_y(\varepsilon_p, \dot{\varepsilon}_p, T) = (A + B{\varepsilon_p}^n)\left(1 + C ln\left(\frac{\dot{\varepsilon}_p}{\dot{\varepsilon}_0}\right)\right)\left(1 - \left(\frac{T - T_{room}}{T_m - T_{room}}\right)^m\right)$$

Material	A(MPa)	B(MPa)	n	m	C	$\varepsilon_0(s^{-1})$	$T_{room}(K)$	$T_{melt}(K)$
Cu-DHP	200	400	0.6	1	0.012	1	296	1083
EN AW-1050	70	48	0.05	1	0.012	1	296	926

3 Numerical Results

The field temperatures are given below. The temperature remains below the melting temperature. Nevertheless, the minimum edge length of the finite elements in the models (45 µm for V82 and 60 µm for V112) could not be fine enough to capture very localised melting zones at the interface.

V82 at 1 µs V82 at 10 µs

V112 at 1 µs V112 at 7 µs

Figure 6 : Temperature fields

Preliminary validations of the numerical results are made by micrographic analysis.

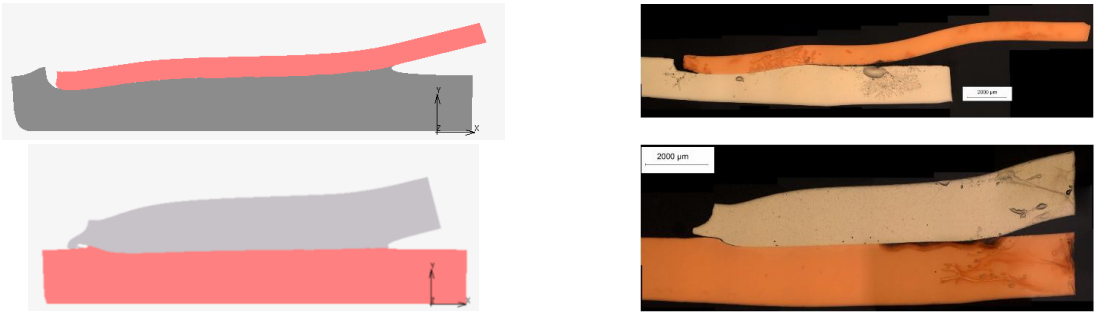

Figure 7: Numerical and experimental deformed shapes

To conclude, our numerical results compare reasonably well with the experimental ones. Improvements regarding contact handling (breakable glue), materials parameters, boundary conditions and mesh refinement could lead to better agreements. Multiphysics simulation to take into account electro-magnetism and meso-scale simulation to capture phenomena occurring at the interface (jet, wavy morphology) will be under investigation soon.

References

[1] V. Psyk&K. Faes “EMW technology”, 2nd Join'Em workshop, Icam, Lille, 7 March 2017.

[2] H. Gallizzi,”Etude et application des champs magnétiques intenses au soudage d’éléments tubulaires en acier oxydables”, Rapport CEA, 1986.

[3] A. Nassiri&al, “Arbitrary Lagrangian–Eulerian finite element simulation and experimental investigation of wavy interfacial morphology during high velocity impact welding,” Mater. Des., vol. 88, pp. 345–358, Dec. 2015.